Energy from spacetime in fluid electrodynamics

M. W. Evans*, H. Eckardt†
Civil List, A.I.A.S. and UPITEC

(www.webarchive.org.uk, www.aias.us,
www.atomicprecision.com, www.upitec.org)

3 Computation, graphics and animation

3.1 Equations inspected

Concerning the numerical solution of equations of fluid dynamics, one has to strictly discern between time-dependent and time-independent (stationary) flows. Time-dependent equations are numerically more stable and therefore easier to handle by finite-element solvers. As discussed in UFT Paper 351, all equations in this paper are homogeneous in the sense that there are no "sourceterms" indepenent of the flux velocity $\mathbf{v}$. This leads to a free floating solution which does not guarantee conservation of mass. Therefore a normalized scalar pressure field p has been added. The divergence of its gradient is assumed to be in proportion to the divergence of the velocity field:

$$\boldsymbol{\nabla} \cdot \boldsymbol{\nabla} p = P \, \boldsymbol{\nabla} \cdot \mathbf{v} \tag{43}$$

with a "penalty constant" P. Then the fundamental vorticity Equation (1) reads:

$$R \frac{\partial \mathbf{v}}{\partial t} + \boldsymbol{\nabla} \times \mathbf{w} + R \, \mathbf{w} \times \mathbf{v} + \boldsymbol{\nabla} p = \mathbf{0}. \tag{44}$$

The equation has been multiplied by R to allow for setting $R = 0$. For comparison we have studied the stationary form of this equation:

$$\boldsymbol{\nabla} \times \mathbf{w} + R \, \mathbf{w} \times \mathbf{v} + \boldsymbol{\nabla} p = \mathbf{0} \tag{45}$$

and another (a priori stationary) vorticity equation derived in note 352(2):

$$\boldsymbol{\nabla} \times \mathbf{w} - R \left(2 \, \mathbf{v} \times \mathbf{w} - \frac{1}{2} \boldsymbol{\nabla} v^2 \right) + \boldsymbol{\nabla} p = \mathbf{0}. \tag{46}$$

*email: emyrone@aol.com
†email: mail@horst-eckardt.de

3.2 Graphics and animation

The time evolution of Eq. (44) converges to a quasi-stationary state. Calculations have been carried out for different values of the Reynolds number R. The sample region is the same as for UFT paper 351. The velocity distribution in the plane $Y = 0$ has been graphed in Figs. 1-3 for parameters $R = 0.1$, 10 and 1000. The velocity maxima change from the output to the input and are distorted in the centre of inlet and outlet for the highest Reynolds number. The behaviour of turbulent structures is best studied by the vorticity $\mathbf{w}$. These are shown for the plane $Z = 0$ in Figs. 4-6 for the three Reynolds numbers. Obviously the structure becomes significantly more irregular for higher Reynolds numbers. It should be noted that the numerical precision is not optimal because of restrictions of the FEM program being available. Therefore results for high Reynolds numbers are not very reliable.

The time dependence of solutions has been processed to animations which will be published on the AIAS web site www.aias.us. The results are not always reproducible, they depend on the size of initial time integration steps. This is an indicator for a chaotic behaviour of solutions. Sometimes divergences appear in the main volume during the first steps of calculation. Then it takes longer to bring them to the inlet side which is the stationary final state. The calculations were always started with the valid solution $\mathbf{v} = \mathbf{0}$.

The other graphs show stationary solutions. The stationary form of Eq.(1), Eq. (45), can be solved for $R = 0$. This is not possible for the time-dependent equation. Comparing this solution (Fig. 7) with Fig. 1, it looks very similar, where the input velocity is even stronger reduced. This picture does not change significantly for Reynolds numbers up to 1000, showing that turbulence is mainly a dynamic effect. The same result was obtained from the equations solved in UFT paper 351.

The remaining graphs present results of Eq. (46), which is essentially an extension of Eq. (45) by a non-linear term. For $R = 0$, both equations give the same result. However, Eq. (46) gives converging solutions only for low Reynolds numbers. In Fig. 8 the velocity distribution for $R = 10$ is shown. In comparison with Fig. 2, the non-linear term leads to an enhancement of the input flow. The reason for this can be seen from Figs. 9 and 10, where the divergence of the velocity is graphed. In the main area of the plane the divergence vanishes, i.e. $\mathbf{v}$ is divergence-free there. Going from $R = 0$ to $R = 10$, the divergence region is relocated from the output to the input region. The vorticity (Figs. 11 and 12) shows a similar tendency, but less pronounced. The same holds for the current density $\mathbf{J}_F$ (Fig. 13-14, based on Eq. (10)).

3.3 Algorithms for deriving electromagnetic properties from flow properties

For future applications it is important to have a line of computing electromagnetic properties directly from the "aether flow field" $\mathbf{v}$. The following two procedures can be carried out. The first is:

1. solve the flow problem for $\mathbf{v}$
2. compute q_F by (3) and ρ_{vac} by (11)

3. compute electric potential ϕ_W by (25) assuming $\boldsymbol{\nabla} \times \mathbf{W} = 0$

4. compute electric field by $\mathbf{E} = -\boldsymbol{\nabla}\phi_W$ (eq. (18) without $\mathbf{W}$)

This seems particularly appropriate in case of electrostatic problems. If a magnetic field is required too, the second procedure is a bit more complicated:

1. compute $\mathbf{J}_F$ by (10) and $\mathbf{J}_{\text{vac}}$ by (12)

2. compute $\mathbf{W}$ by (30) where $\mathbf{J}_{\text{vac}}$ is used on the RHS

3. compute magnetic induction $\mathbf{B}$ by (17)

Alternatively, one could solve the Maxwell-Heaviside-like equations (20) and (22) directly with vacuum current on the right-hand side. Then the solution is fully time-dependent by definition and computation of potentials is avoided. Thus the aether problem is reduced to computing a (time-dependent) vacuum current density and all electrical properties will follow. Practical results will be given in later papers because volume definitions and boundary conditions for meaningful physical situations have to be developed first.

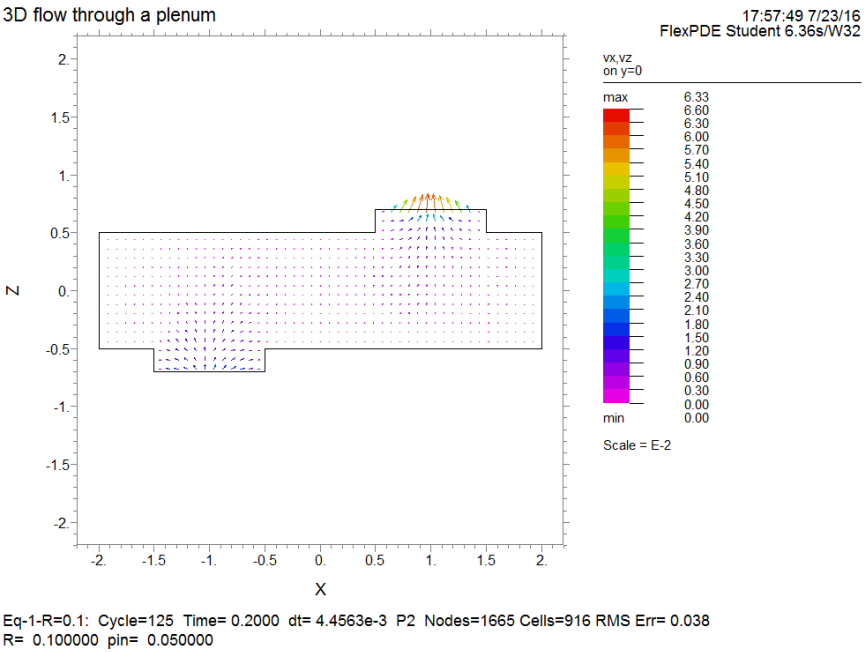

Figure 1: Velocity solution of Eq. (44) for $R = 0.1$.

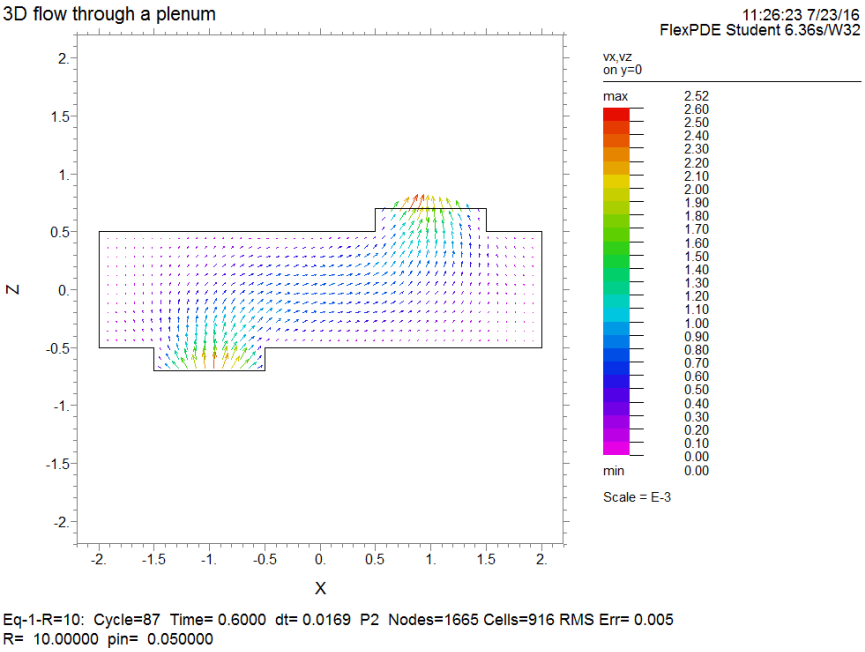

Figure 2: Velocity solution of Eq. (44) for $R = 10$.

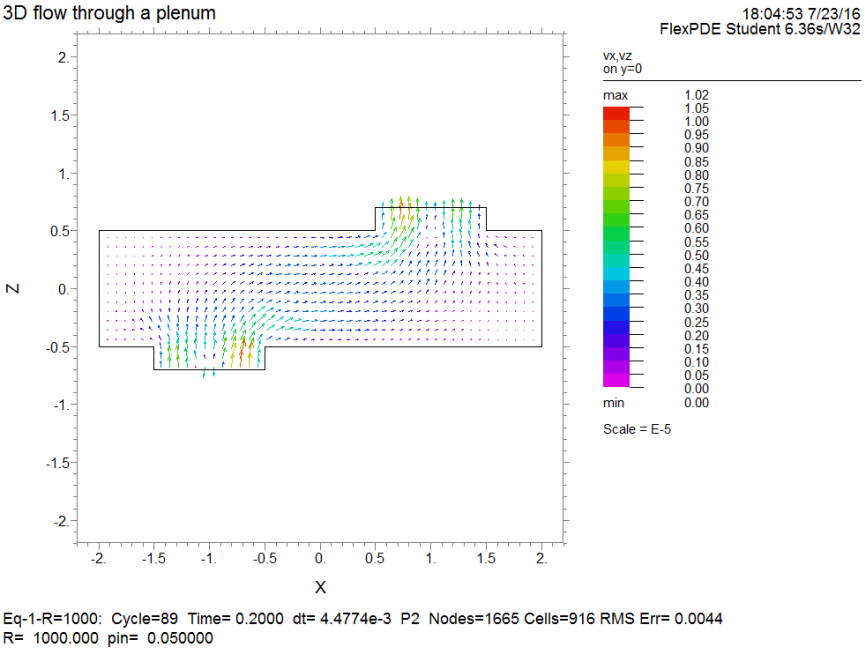

Figure 3: Velocity solution of Eq. (44) for $R = 1000$.

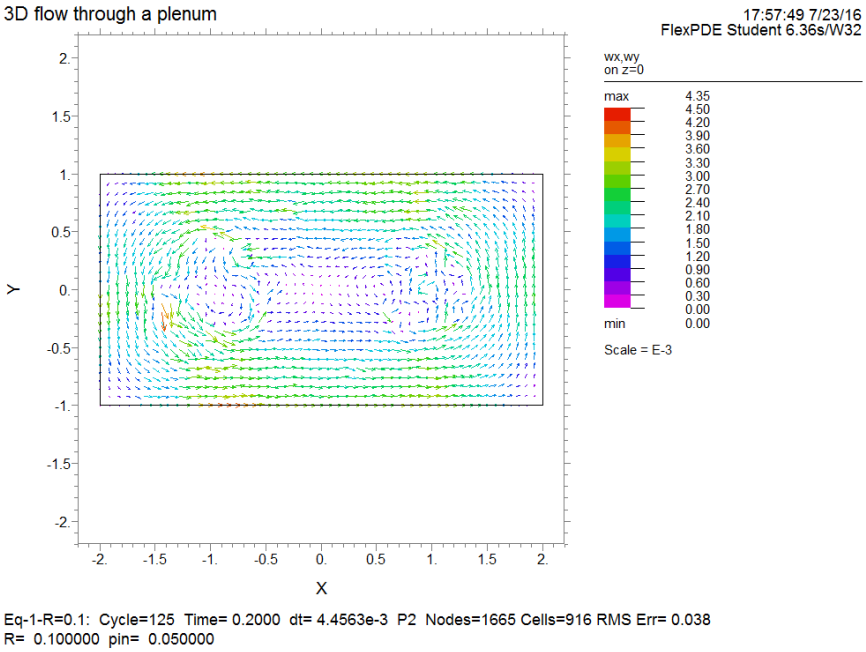

Figure 4: Vorticity from Eq. (44) for $R = 0.1$.

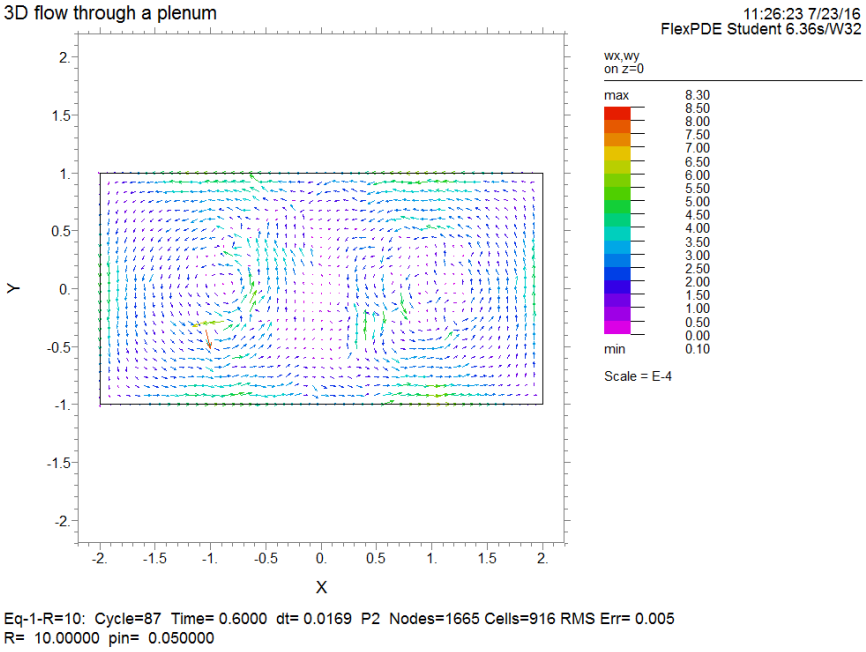

Figure 5: Vorticity from Eq. (44) for $R = 10$.

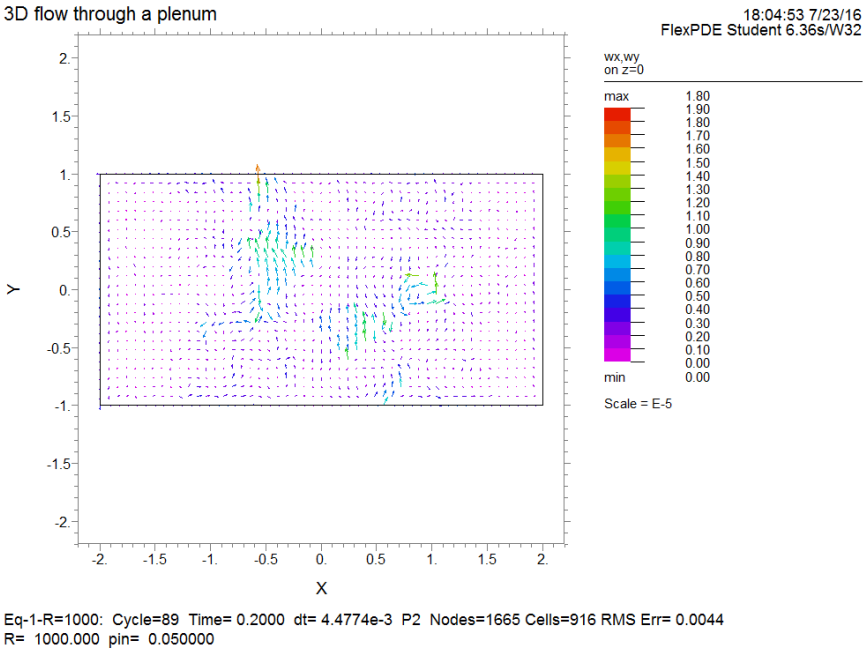

Figure 6: Vorticity from Eq. (44) for $R = 1000$.

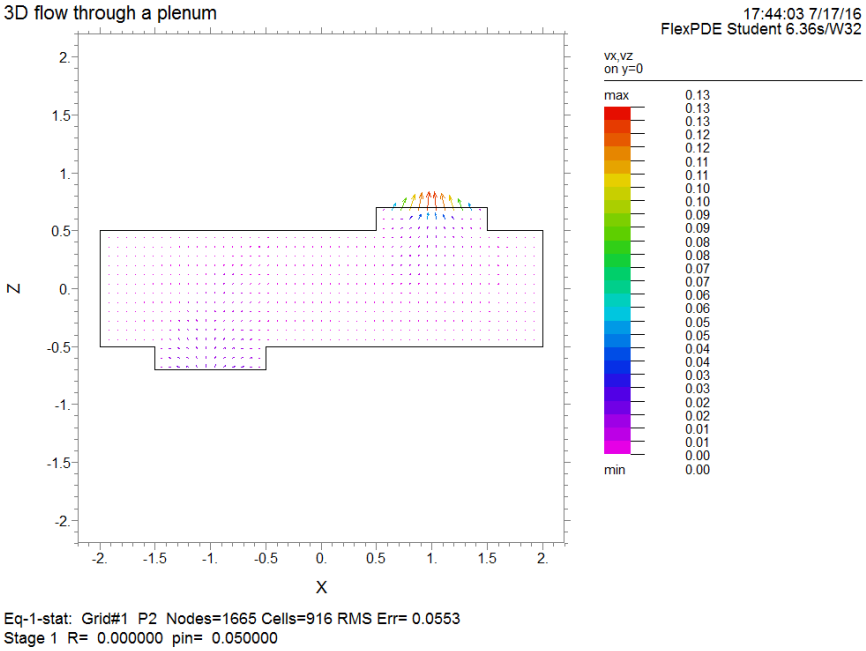

Figure 7: Velocity solution of static Eq. (45).

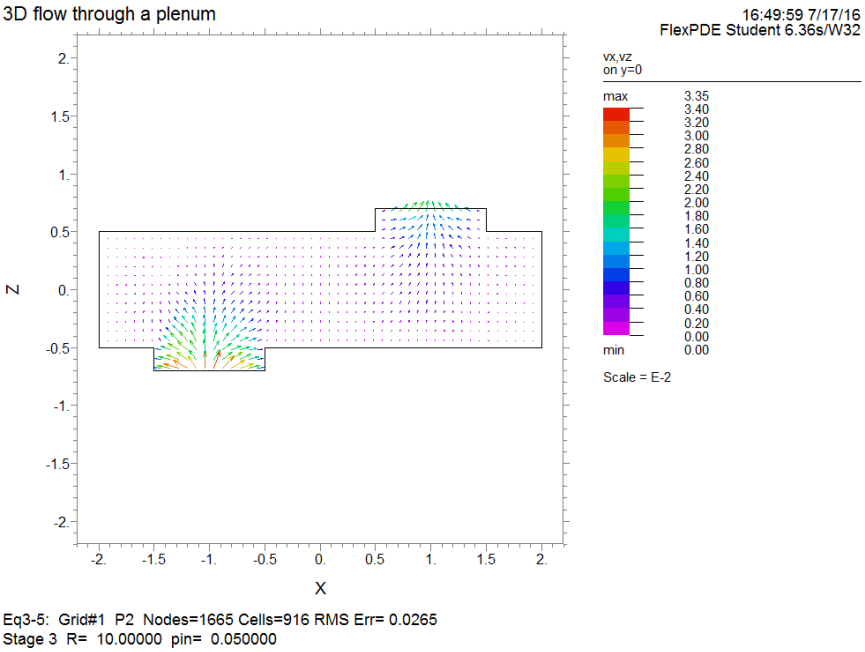

Figure 8: Velocity solution of (46) for $R = 10$.

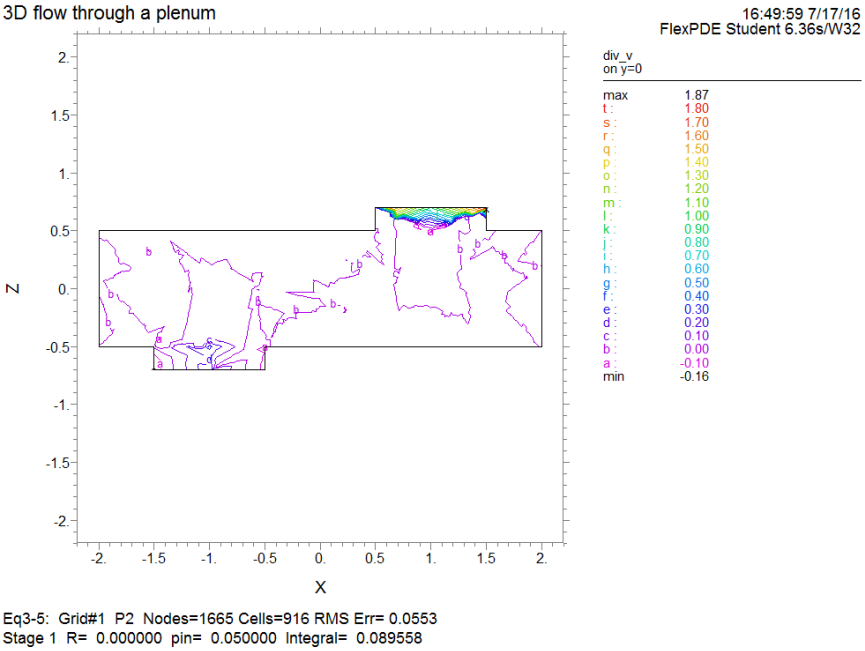

Figure 9: Divergence of velocity from Eq. (46) for $R = 0$.

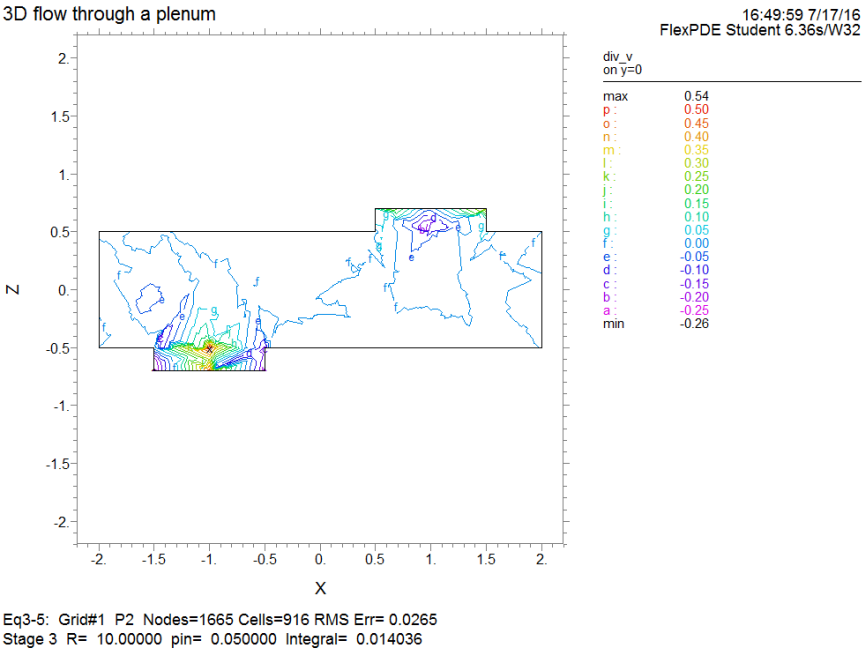

Figure 10: Divergence of velocity from Eq. (46) for $R = 10$.

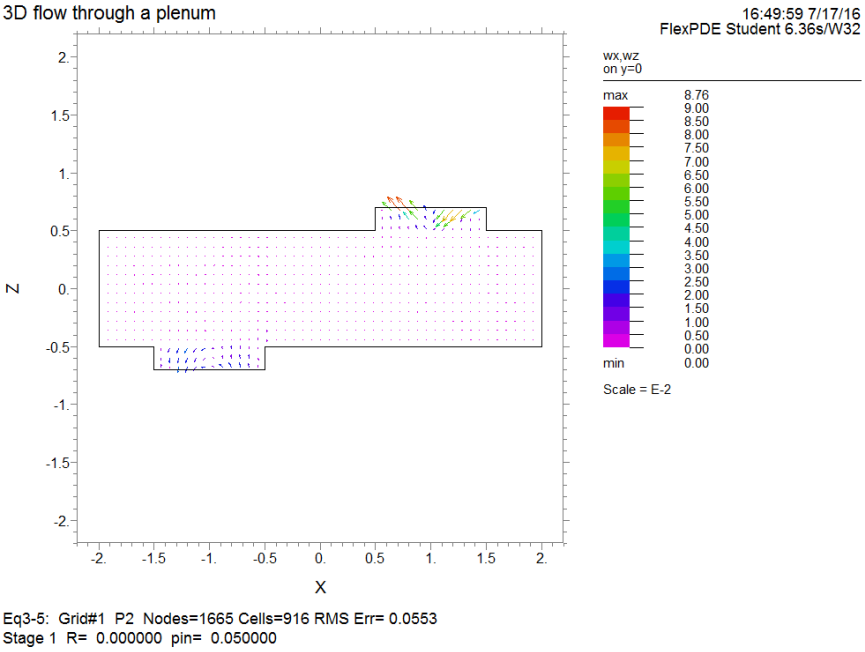

Figure 11: Vorticity from Eq. (46) for $R = 0$.

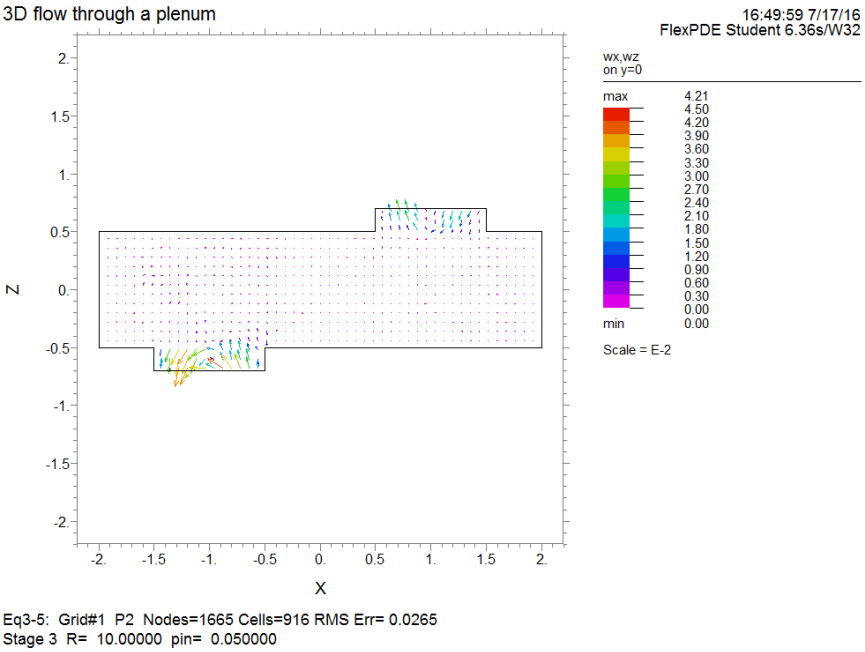

Figure 12: Vorticity from Eq. (46) for $R = 10$.

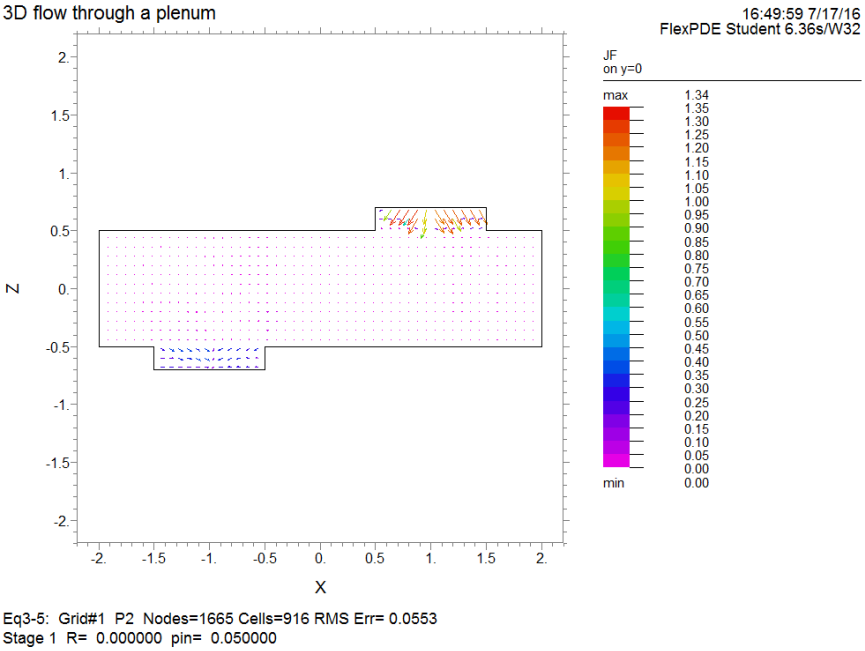

Figure 13: Current density $\mathbf{J}_F$ from Eq. (46) for $R = 0$.

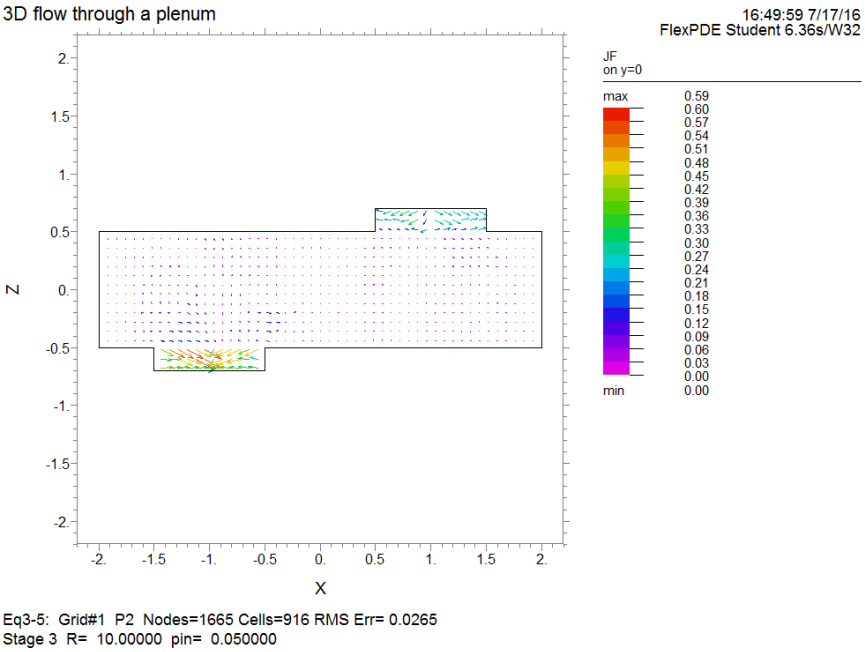

Figure 14: Current density $\mathbf{J}_F$ from Eq. (46) for $R = 10$.